JOURNAL OF SOLID STATE CHEMISTRY 111, 52–57 (1994)

Determination of Complex Structures from Powder Diffraction Data: The Crystal Structure of $La_3Ti_5Al_{15}O_{37}$

Russell E. Morris*,† Jonathan J. Owen,* Judith K. Stalick,† and Anthony K. Cheetham*

* *Materials Department, University of California, Santa Barbara, California 93106; and † Reactor Radiation Division, National Institute of Standards and Technology, Gaithersburg, Maryland 20899*

Received January 10, 1994; Accepted February 14, 1994
IN HONOR OF C.N.R. RAO ON HIS 60TH BIRTHDAY

The applicability of powder diffraction techniques to structure determination has improved substantially in recent times, but it has only been successfully utilized in the solution of relatively simple structures of up to 29 atoms in the asymmetric unit. The structure $La_3Ti_5Al_{15}O_{37}$, which has 60 atoms in the asymmetric unit, has been solved using a combination of synchrotron X-ray and neutron powder diffraction. This represents a considerable advance in the size of structure that has been solved using powder diffraction techniques. The structure of $La_3Ti_5Al_{15}O_{37}$ consists of small regions of simpler structure types in the La/Ti/Al/O system, interleaved to form a complex 3D network. © 1994 Academic Press, Inc.

INTRODUCTION

A substantial number of important materials, both organic and inorganic, cannot be obtained in a form that is suitable for structural characterization by single-crystal X-ray methods. These materials include many zeolites, electronic materials, ceramics, and important biological molecules such as peptides. This state of affairs has stimulated remarkable progress during the past decade in the development of methods for the determination of structures from powder diffraction data. As a result of important advances with laboratory X rays (1), neutrons (2), and synchrotron X rays (3), in the mid-1980s, the solution and refinement of structures with up to 20 atoms in the asymmetric unit have become quite routine (4). The most complex structures that have been solved to date by using these methods are $Ga_2(HPO_3)_3 \cdot 4H_2O$ (5) and β-Ba_3AlF_9 (6), both of which have 29 independent atoms. These structures appear to have represented the limit of what might be solved and refined from powder data, but we now show that a structure of twice this complexity can be solved by harnessing the combined powers of X-ray and neutron powder techniques.

$La_3Ti_5Al_{15}O_{37}$ belongs to a class of materials that are difficult to prepare (7). In this instance, the difficulty probably stems from its close similarity to related, but simpler, structures, and to the narrow temperature range within which it can be synthesized. On the other hand, it is a very interesting phase, both on account of its possible role in radwaste disposal and its relationship to phases that might be implicated in the evolution of solar nebulas (7, 8). Even under conditions where a compound such as $La_3Ti_5Al_{15}O_{37}$ is the thermodynamically stable product, the nucleation barrier to the formation of the more complex phase may be high relative to the simpler structure types. Under such conditions, it seems highly unlikely that materials of this type will be prepared as single crystals.

SYNTHESIS

The synthetic conditions needed to make $La_3Ti_5Al_{15}O_{37}$ were first reported by Morgan (7), where the compound was formulated as $LaTi_2Al_9O_{19}$. In the present work, γ-AlOOH was prepared by drying the gelatinous precipitate obtained by addition of NaOH to a solution of $AlCl_3$. The γ-AlOOH was dispersed in *i*-PrOH (isopropanol), to which $Ti(i\text{-}OPr)_4$ was added, followed by $La(NO_3)_3$ in 5 ml of water (quantities were such that the molar ratios of La : Ti : Al were 1 : 2 : 9). The mixture was heated to remove the isopropanol and nitrate, and the product was then pressed into pellets which were placed in an alumina crucible and heated from 800 to 1350°C at 1°C min^{-1}. The alumina crucible was placed on a bed of $CaCO_3$ to prevent any contamination of the product by Mo from the furnace elements. The reaction mixture was left at 1350°C for 3 days and then cooled rapidly in the furnace. $La_3Ti_5Al_{15}O_{37}$ was recovered as a white, microcrystalline powder. A laboratory X-ray diffraction study indicated that a small quantity of rutile was also present in the powder. The unit cell could be indexed as monoclinic C-centered with $a = 22.54$ Å, $b = 10.97$ Å, $c = 9.67$ Å, and $\beta = 98.49°$, with systematic absences consistent with spacegroups $C2/c$ or Cc. The powder pattern is the same as those reported for $LaTi_2Al_9O_{19}$ and $SrTi_3Al_8O_{19}$ (9).

0022-4596/94 $6.00

STRUCTURE DETERMINATION

A room temperature synchrotron X-ray powder diffraction pattern was collected on station 9.1 at the Synchrotron Radiation Source, Daresbury, UK. The wavelength used in the experiment was 1.0000(2) Å, selected using a Si(111) monochromator. Data collection was accomplished with the sample on a flat plate over an angular range of $6° < 2\theta < 70°$. Integrated intensities were obtained by using the Le Bail adaptation (10) of the Rietveld method (11) in the GSAS (12) suite of programs; the least-squares refinement included terms for background, lattice parameters (for both $La_3Ti_5Al_{15}O_{37}$ and rutile), diffractometer zero point, and a pseudo-Voigt peak shape, and converged to final agreement factors of $R_p = 7.96\%$ and $R_{wp} = 14.45\%$ (Fig. 1). There was no evidence from the refined peak shape of any sample line-broadening effects, indicating that the resolution was essentially instrument limited. Structure factors for 1902 reflections were extracted and input into the direct methods program MULTAN84 (13). No chemically sensible solution could be found in spacegroup $C2/c$, and all subsequent calculations were carried out in spacegroup Cc. The initial structure solution involved the estimation and refinement of the phases associated with the 205 largest $|E|$ values and used 1977 triplet relationships. The figures of merit for the best solution were ABSFOM = 1.087, $\Psi_0 = 2.350$ (from 149 phase relationships using the 100 weakest $|E|$ values), and RESID = 6.19, with a MULTAN84 combined figure of merit = 2.555. The E map produced by this solution showed five large peaks, split into two groups according to their peak height, and these were assigned as 3 lanthanum and 2 titanium atoms. Difference Fourier syntheses then revealed the positions of 9 more metal atoms, which were initially assigned as aluminium, and 27 oxygen atoms. At this point, however, Fourier syntheses failed to reveal any of the remaining atoms.

A 3-g sample of $La_3Ti_5Al_{15}O_{37}$ was prepared and neutron powder data were collected on the 32-detector diffractometer BT-1 at the National Institute of Standards and Technology, Gaithersburg, Maryland. The wavelength used was 1.539(1) Å, selected using a Cu(311) monochromator and 15′,20′,7′ collimation. No impurities were evident in the new sample. The subsequent Rietveld refinement utilized data in the range $20° < 2\theta < 140°$; high- and low-angle regions were excluded because of high background. Difference Fourier syntheses revealed the positions of the remaining 10 oxygen atoms and 7 more aluminium atoms. Careful inspection of the atoms showed that one of the metal atoms that was found from the synchrotron data was incorrectly assigned as aluminium and was replaced by a titanium atom. From a final difference Fourier synthesis, the last 2 titanium atoms could be located. Full Rietveld refinement proceeded to a satisfactory profile fit, but in order to improve the precision of the refinement another neutron powder diffraction data set was collected on the same sample, this time using a Si(531) monochromator and a wavelength of

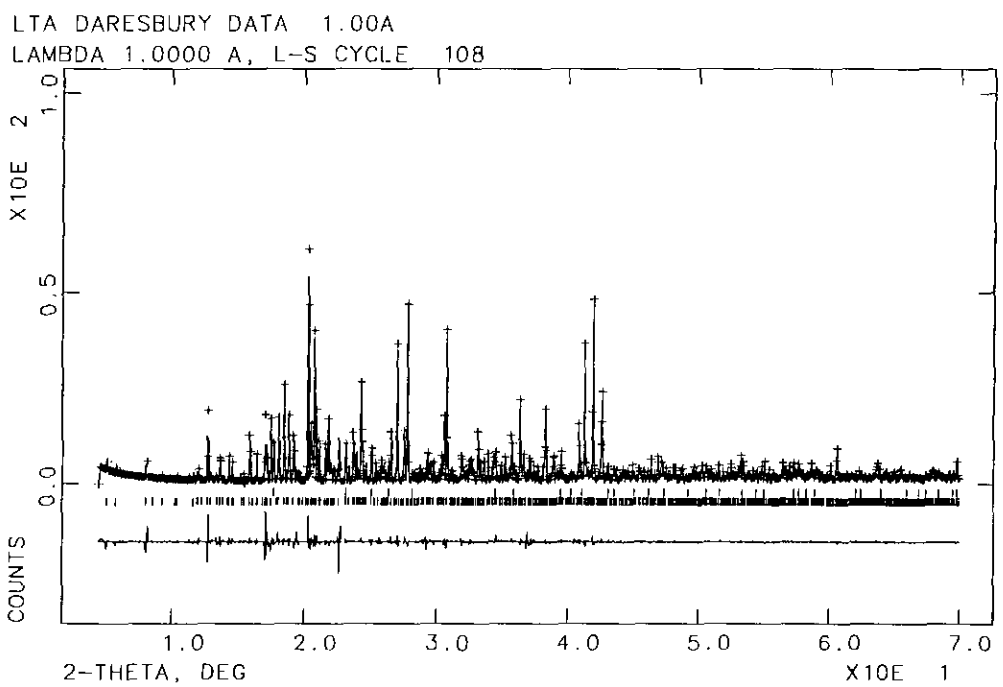

FIG. 1. Observed, calculated, and difference plots for the Le Bail modified Rietveld refinement of $La_3Ti_5Al_{15}O_{37}$ against synchrotron X-ray data. Tick marks show the position of reflections for both the $La_3Ti_5Al_{15}O_{37}$ and rutile phases.

TABLE 1
Final Fractional Atomic Coordinates and Isotropic Temperature Factors for $La_3Ti_5Al_{15}O_{37}$

	x	y	z	U_{iso}/Å^2
La(1)	0.47900	0.6268(23)	0.41200	0.013(2)
La(2)	0.3586(10)	0.6324(22)	0.0470(28)	0.013(2)
La(3)	0.7716(12)	0.1156(21)	0.6723(35)	0.013(2)
Ti(1)	0.5130(18)	0.882(4)	0.632(4)	0.020(3)
Ti(2)	0.4221(26)	0.395(5)	0.254(6)	0.020(3)
Ti(3)	0.3075(29)	0.647(7)	0.341(7)	0.020(3)
Ti(4)	0.128(4)	0.745(8)	0.366(7)	0.020(3)
Ti(5)	0.6293(34)	0.982(7)	0.863(8)	0.020(3)
Al(1)	0.6170(21)	0.900(4)	0.623(5)	0.007(1)
Al(2)	0.0279(19)	0.7630(30)	0.327(4)	0.007(1)
Al(3)	0.3840(17)	0.875(4)	0.378(4)	0.007(1)
Al(4)	0.4193(19)	0.8979(34)	0.690(4)	0.007(1)
Al(5)	0.3305(17)	1.010(4)	0.615(4)	0.007(1)
Al(6)	0.5266(24)	0.989(5)	0.837(5)	0.007(1)
Al(7)	0.4490(15)	0.882(4)	0.059(4)	0.007(1)
Al(8)	0.1957(18)	0.121(5)	0.151(5)	0.007(1)
Al(9)	0.2274(16)	0.7563(29)	0.060(4)	0.007(1)
Al(10)	0.0282(17)	0.111(4)	0.077(4)	0.007(1)
Al(11)	0.3123(18)	0.1349(35)	0.341(4)	0.007(1)
Al(12)	0.1935(16)	0.0233(31)	0.404(4)	0.007(1)
Al(13)	0.1226(17)	0.3642(33)	0.140(4)	0.007(1)
Al(14)	0.1003(15)	0.8571(28)	0.103(4)	0.007(1)
Al(15)	0.1203(25)	0.245(6)	0.343(6)	0.007(1)
O(1)	0.4703(16)	0.9932(26)	0.663(4)	0.008(1)
O(2)	0.4611(12)	0.8768(28)	0.4016(32)	0.008(1)
O(3)	0.5702(12)	0.8801(20)	0.7634(30)	0.008(1)
O(4)	0.5661(15)	1.0011(26)	0.522(4)	0.008(1)
O(5)	0.5669(15)	0.7495(22)	0.5275(33)	0.008(1)
O(6)	0.4748(17)	0.7534(27)	0.665(4)	0.008(1)
O(7)	0.3643(12)	−0.0067(28)	0.2685(33)	0.008(1)
O(8)	0.4678(12)	0.3613(23)	0.4070(32)	0.008(1)
O(9)	0.3737(13)	0.4985(23)	−0.2013(29)	0.008(1)
O(10)	0.3698(15)	0.6337(27)	0.544(4)	0.008(1)
O(11)	0.3736(15)	0.2338(27)	0.2960(34)	0.008(1)
O(12)	0.4737(14)	0.5030(22)	0.1533(33)	0.008(1)
O(13)	0.3740(14)	0.8809(25)	0.5412(30)	0.008(1)
O(14)	0.3703(12)	0.7467(21)	0.2733(28)	0.008(1)
O(15)	0.3681(16)	0.8666(25)	0.0115(33)	0.008(1)
O(16)	0.4708(14)	0.8748(25)	−0.1120(35)	0.008(1)
O(17)	0.4708(15)	0.7324(24)	0.1105(33)	0.008(1)
O(18)	0.5774(15)	0.1223(27)	0.7610(34)	0.008(1)
O(19)	0.2749(17)	0.7547(26)	0.425(4)	0.008(1)
O(20)	0.2817(13)	0.6236(26)	0.167(4)	0.008(1)
O(21)	0.2776(14)	0.4869(24)	0.4209(31)	0.008(1)
O(22)	0.2689(15)	0.0055(27)	0.413(4)	0.008(1)
O(23)	0.2733(14)	0.1333(26)	0.664(4)	0.008(1)
O(24)	0.2742(14)	0.8762(25)	0.6667(35)	0.008(1)
O(25)	0.0711(13)	0.1313(26)	0.2829(34)	0.008(1)
O(26)	0.0694(16)	0.2444(27)	0.026(4)	0.008(1)
O(27)	0.0721(13)	−0.0030(25)	0.0078(32)	0.008(1)
O(28)	0.1769(13)	0.5066(26)	0.2096(32)	0.008(1)
O(29)	0.1739(17)	0.4120(25)	0.464(4)	0.008(1)
O(30)	0.1720(15)	0.2514(23)	0.2290(31)	0.008(1)
O(31)	0.2720(14)	0.2526(24)	0.4249(34)	0.008(1)
O(32)	0.1733(15)	0.6255(30)	0.4521(33)	0.008(1)
O(33)	0.1731(14)	−0.0112(24)	0.2269(34)	0.008(1)
O(34)	0.1689(13)	0.1420(20)	0.4803(33)	0.008(1)
O(35)	0.1737(14)	0.1155(25)	−0.0331(33)	0.008(1)
O(36)	0.1739(15)	0.7604(26)	0.226(4)	0.008(1)
O(37)	0.0780(15)	0.8662(24)	0.2807(34)	0.008(1)

1.589 Å. The higher take-off angle for the Si(531) crystal compared with the Cu(311) monochromator yields greater resolution toward the high-angle end of the diffraction pattern.

A joint Rietveld refinement was carried out using both the Cu(311) and Si(531) data sets. The angle range for the Si(531) data was $10° < 2\theta < 160°$. The light scatterers, aluminium and titanium, were rather unstable in the early stages of atomic position refinement, and soft constraints were needed to prevent chemically unreasonable metal–metal bond distances. As the refinement neared convergence, however, the restraints were lifted, except for those relating to the tetrahedrally coordinated aluminum atoms, yielding the final atomic parameters shown in Table 1. The unit cell refined to $a = 22.5655(3)$ Å, $b = 10.9863(2)$, $c = 9.7189(1)$ Å, and $\beta = 98.569(2)°$. Final agreement factors for the two-data-set refinement were $R_{wp} = 8.79\%$, $R_p = 6.68\%$, R_F(Cu(311)) 6.69%, R_F(Si(531)) = 7.68%, and $\chi = 2.3$. Observed, calculated, and difference profiles for the two data sets in the joint refinement are shown in Figs. 2 and 3.

The space group, *Cc*, is polar in the *a* and *c* directions, and in order to fix the origin of the structure the La(1) *x* and *z* coordinates were left unrefined. The isotropic temperature factors, U_{iso}, for each elemental type are constrained to be equal. Final bond distances are given in Table 2. The program MISSYM (14), which tests a model for any symmetry elements that are not accounted for in the space group, found that the atomic positions were only related by the space group symmetry and thus the best description of the structure is indeed in the noncentrosymmetric space group *Cc*. In complicated structures of this kind, with large numbers of independently refineable parameters, loss of information because of peak overlap in the diffraction pattern inevitably leads to poor accuracy in the positions of some atoms, especially the lighter scatterers. Nevertheless, the essential features of the structure are clearly revealed. One way to improve the refinement would be to add further observations in the form of "soft constraints" on the bond distances, but because of the irregular nature of the coordination polyhedra expected around La, Ti, and nontetrahedral Al, no other observations were added (15).

DISCUSSION

$La_3Ti_5Al_{15}O_{37}$ (Fig. 4) consists of columns of $La_2Ti_2O_7$ interleaved with regions of $LaAlO_3$- and Al_2TiO_5-type structures. The highly coordinated lanthanum atoms (2 × 12 and 1 × 11 coordinate) show some similarity to those found in the perovskite-related phase $La_2Ti_2O_7$. These lanthanum coordination polyhedra are then linked via the sharing of faces to three of the TiO_6 units (those containing Ti(1), Ti(2) and Ti(3)); the latter units are distorted in a similar fashion to those seen in $La_2Ti_2O_7$ (16), with three

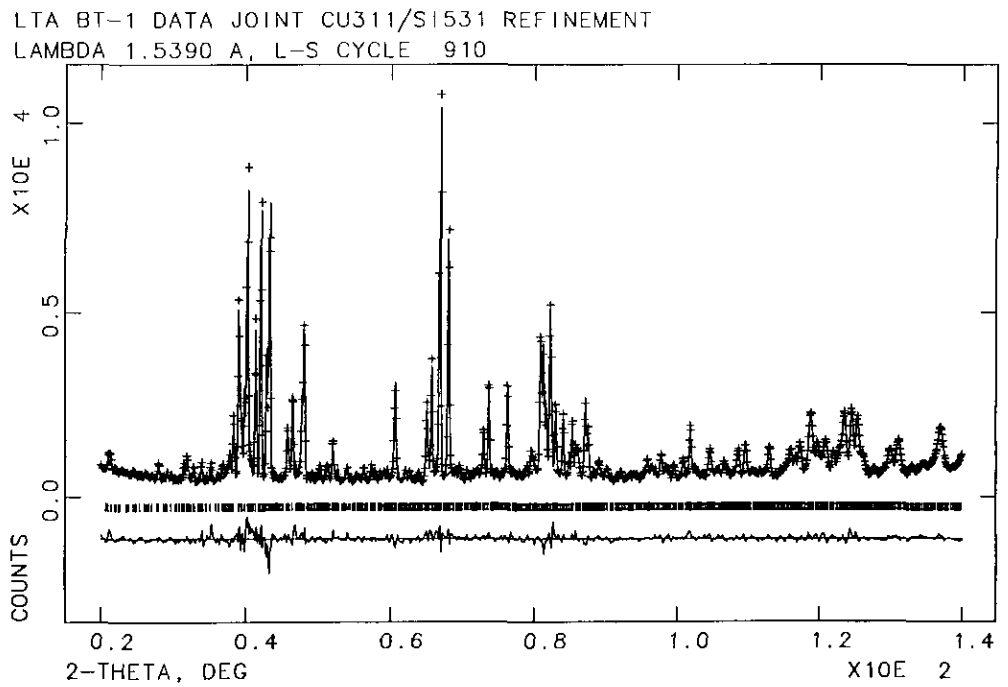

FIG. 2. Observed, calculated, and difference plots for the joint Rietveld refinement against neutron data (Cu(311) monochromator, λ = 1.539 Å).

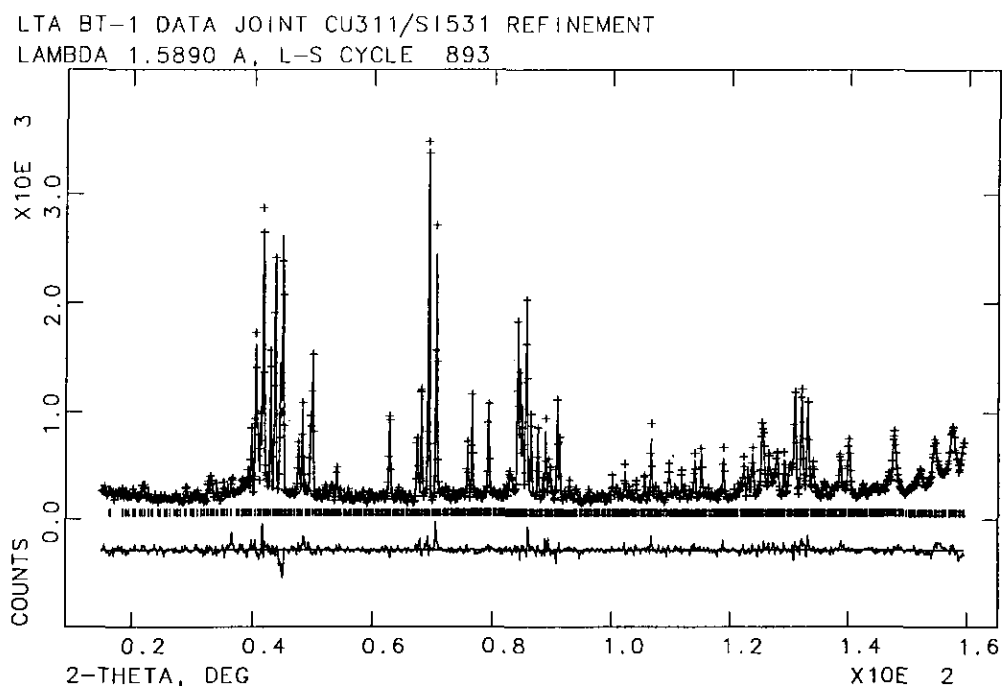

FIG. 3. Observed, calculated, and difference plots for the joint Rietveld refinement against neutron data (Si(531) monochromator, λ = 1.589 Å).

TABLE 2
Bond Distances (with e.s.d's) for $La_3Ti_5Al_{15}O_{37}$

Bond	Distance	Bond	Distance
La(1)–O(2)	2.78(4)	La(2)–O(8)	2.988(27)
La(1)–O(5)	2.520(33)	La(2)–O(9)	2.890(31)
La(1)–O(6)	2.83(4)	La(2)–O(9)	2.814(29)
La(1)–O(8)	2.928(34)	La(2)–O(10)	2.93(4)
La(1)–O(9)	2.823(32)	La(2)–O(11)	2.910(32)
La(1)–O(10)	2.944(33)	La(2)–O(12)	3.005(29)
La(1)–O(12)	2.846(32)	La(2)–O(14)	2.512(30)
La(1)–O(12)	2.762(34)	La(2)–O(15)	2.609(34)
La(1)–O(14)	2.930(27)	La(2)–O(17)	2.743(32)
La(1)–O(25)	2.584(31)	La(2)–O(20)	2.230(30)
La(1)–O(27)	2.558(30)	La(2)–O(21)	2.427(32)
		La(2)–O(31)	2.477(31)
La(3)–O(28)	2.594(29)	Ti(1)–O(1)	1.61(5)
La(3)–O(9)	2.763(29)	Ti(1)–O(2)	2.37(4)
La(3)–O(10)	2.706(34)	Ti(1)–O(3)	1.68(4)
La(3)–O(11)	2.943(34)	Ti(1)–O(4)	2.16(5)
La(3)–O(19)	2.862(34)	Ti(1)–O(5)	2.23(5)
La(3)–O(20)	2.64(4)	Ti(1)–O(6)	1.71(6)
La(3)–O(21)	2.844(32)		
La(3)–O(21)	2.650(31)	Ti(2)–O(6)	2.27(6)
La(3)–O(24)	2.86(4)	Ti(2)–O(8)	1.72(6)
La(3)–O(32)	2.846(34)	Ti(2)–O(9)	1.70(6)
La(3)–O(30)	2.803(32)	Ti(2)–O(10)	2.22(6)
La(3)–O(31)	2.850(35)	Ti(2)–O(11)	2.15(6)
		Ti(2)–O(12)	2.01(6)
Ti(3)–O(9)	2.27(7)	Ti(4)–O(3)	2.04(8)
Ti(3)–O(10)	2.26(7)	Ti(4)–O(26)	2.18(9)
Ti(3)–O(14)	1.98(7)	Ti(4)–O(35)	2.02(8)
Ti(3)–O(19)	1.67(7)	Ti(4)–O(36)	1.85(8)
Ti(3)–O(20)	1.73(7)	Ti(4)–O(32)	1.79(9)
Ti(3)–O(21)	2.08(8)	Ti(4)–O(37)	1.86(8)
Ti(5)–O(28)	1.97(8)	Al(1)–O(28)	1.80(5)
Ti(5)–O(29)	1.74(9)	Al(1)–O(29)	2.15(5)
Ti(5)–O(3)	1.89(8)	Al(1)–O(3)	1.86(5)
Ti(5)–O(4)	2.26(8)	Al(1)–O(4)	1.78(5)
Ti(5)–O(18)	2.09(8)	Al(1)–O(5)	2.14(5)
Ti(5)–O(32)	1.70(8)	Al(1)–O(36)	2.32(5)
Al(2)–O(3)	1.99(4)		
Al(2)–O(6)	1.84(4)	Al(3)–O(2)	1.74(4)
Al(2)–O(8)	1.98(4)	Al(3)–O(7)	1.69(4)
Al(2)–O(16)	2.13(4)	Al(3)–O(13)	1.68(4)
Al(2)–O(26)	2.02(4)	Al(3)–O(14)	1.69(4)
Al(2)–O(37)	1.71(4)		
Al(4)–O(1)	1.61(5)	Al(5)–O(7)	1.57(4)
Al(4)–O(6)	2.06(4)	Al(5)–O(13)	1.92(5)
Al(4)–O(7)	1.96(5)	Al(5)–O(15)	1.95(5)
Al(4)–O(11)	2.13(5)	Al(5)–O(22)	2.23(4)
Al(4)–O(13)	1.65(4)	Al(5)–O(23)	1.98(4)
Al(4)–O(16)	2.11(4)	Al(5)–O(24)	2.06(5)
Al(6)–O(1)	1.96(5)		
Al(6)–O(2)	2.24(6)	Al(7)–O(1)	1.77(4)
Al(6)–O(3)	1.77(6)	Al(7)–O(15)	1.78(4)
Al(6)–O(4)	1.89(5)	Al(7)–O(16)	1.78(3)
Al(6)–O(16)	1.90(6)	Al(7)–O(17)	1.78(5)
Al(6)–O(18)	2.06(6)		

TABLE 2—*Continued*

Bond	Distance	Bond	Distance
		Al(9)–O(29)	2.33(4)
Al(8)–O(24)	1.75(4)	Al(9)–O(20)	2.08(4)
Al(8)–O(33)	1.75(5)	Al(9)–O(23)	1.80(4)
Al(8)–O(35)	1.75(4)	Al(9)–O(34)	1.815(34)
Al(8)–O(30)	1.74(6)	Al(9)–O(36)	2.15(4)
		Al(9)–O(31)	1.77(4)
Al(10)–O(8)	2.00(4)	Al(11)–O(7)	2.13(5)
Al(10)–O(12)	1.94(4)	Al(11)–O(11)	1.86(5)
Al(10)–O(17)	1.92(5)	Al(11)–O(15)	1.93(4)
Al(10)–O(25)	2.10(4)	Al(11)–O(22)	1.92(5)
Al(10)–O(26)	1.84(5)	Al(11)–O(24)	1.78(4)
Al(10)–O(27)	1.79(5)	Al(11)–O(31)	1.84(5)
		Al(13)–O(28)	2.04(4)
Al(12)–O(22)	1.71(4)	Al(13)–O(4)	2.17(4)
Al(12)–O(33)	1.70(4)	Al(13)–O(18)	1.67(4)
Al(12)–O(34)	1.67(4)	Al(13)–O(26)	2.00(5)
Al(12)–O(35)	1.72(4)	Al(13)–O(32)	2.30(4)
		Al(13)–O(30)	1.80(4)
Al(14)–O(5)	1.52(4)	Al(15)–O(5)	2.30(5)
Al(14)–O(27)	1.86(4)	Al(15)–O(18)	1.87(6)
Al(14)–O(33)	2.38(4)	Al(15)–O(25)	1.71(6)
Al(14)–O(34)	2.09(4)	Al(15)–O(34)	1.95(6)
Al(14)–O(36)	2.17(4)	Al(15)–O(30)	1.73(6)
Al(14)–O(37)	1.87(4)		

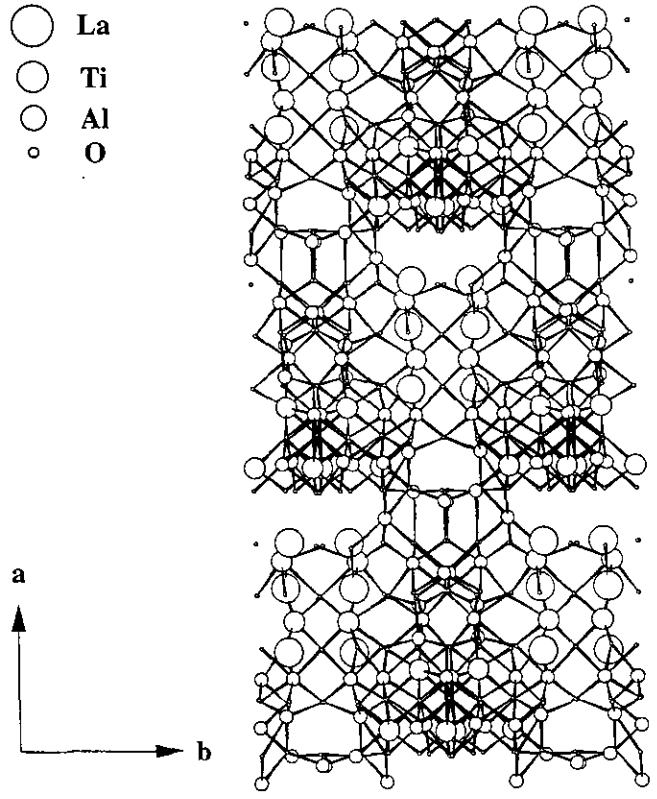

FIG. 4. The structure of $La_3Ti_5Al_{15}O_{37}$ viewed parallel to the *c* axis. Represented are La, Ti, Al, O atoms as circles of decreasing size. La–O bonds are not drawn.

long Ti–O and three short Ti–O bonds. The other two TiO_6 groups are less distorted. There are 4 four-coordinated, 10 six-coordinated, and 1 five-coordinated aluminium atoms present in the structure. The five- and six-coordinated units are distorted from regular polyhedra, as would be expected in a dense aluminium oxide phase containing groups that share faces with each other. However, the polyhedra that contain Al(1), Al(5), Al(6), Al(9), Al(13), Al(14), and Al(15) are distorted to a greater degree than any of the others, and they have long Al–O bonds (~2.2–2.3 Å), similar to those seen in the pseudobrookite structure of Al_2TiO_5 (17), The rest of the material can be described as being distorted $LaAlO_3$ (18), although the lack of precision makes description of smaller distortions in the polyhedral geometries very difficult.

The prediction of Morgan (7) that the structure of $La_3Ti_5Al_{15}O_{37}$ should contain elements of the structures of simpler materials such as pyrochlore and pseudobrookite is borne out by this experiment, although our findings are at variance with the expectation, based upon the stoichiometry and the c lattice parameter of ~22 Å, that the lanthanum atoms would be arranged in layers, as in the β-alumina and magnetoplumbite structures. There are, however, some similarities to the structure of the magnetoplumbite-type lanthanum hexaaluminates (19, 20), especially the presence of four-, five-, and six-coordinate aluminum.

The arrangement of the rare-earth ions leads us to suggest that the magnetic properties of $La_3Ti_5Al_{15}O_{37}$ might be of interest, especially if some or all of the aluminiums were to be substituted by iron. In this respect, the structure is also reminiscent of the garnet system. Furthermore, on the basis of the correct stoichiometry of the lanthanum phase, we can predict the stoichiometry of the strontium phase to be $Sr_3Ti_8Al_{12}O_{37}$ rather than $SrTi_3Al_8O_{19}$. The fresh insight that now becomes possible as a result of determining the structure of $La_3Ti_5Al_{15}O_{37}$ amply illustrates the need for the further development of tools for the determination of structures of powder samples. However, the refinement of structures of greater complexity than $La_3Ti_5Al_{15}O_{37}$ will certainly require the extensive use of soft constraints, as was illustrated in recent work on the SAPO-40 molecular sieve (21).

ACKNOWLEDGMENTS

We thank Drs. Peter Morgan and Jack Rush for useful discussions. This work was supported by the MRL Program of the National Science Foundation under award DMR-9123048

REFERENCES

1. P. Rudolf and A. Clearfield, *Acta Crystallogr. B* **41,** 418 (1985).
2. A. K. Cheetham, A. W. Sleight, M. M. Eddy, R. J. B. Jakeman, M. M. Johnson, and C. C. Torardi, *Nature* **320,** 46 (1986).
3. J. P. Attfield, A. W. Sleight, and A. K. Cheetham, *Nature* **322,** 630 (1986).
4. A. P. Wilkinson and A. K. Cheetham, *Angew. Chem. Int. Ed.* **31,** 1557 (1992).
5. R. E. Morris, W. T. A. Harrison, J. M. Nicol, A. P. Wilkinson, and A. K. Cheetham, *Nature* **359,** 519 (1992).
6. A. Le Bail, *J. Solid State Chem.* **103,** 287 (1993).
7. P. E. D. Morgan, *Mater. Res. Bull.* **19,** 377 (1984).
8. M. Bar-Matthews, I. D. Hutcheon, G. J. MacPherson, and L. Grossman, *Geochim. Cosmochim. Acta* **46,** 31 (1982).
9. H. W. Zandbergen and D. J. W. Ijdo, *Mater. Res. Bull.* **18,** 371 (1983).
10. A. Le Bail, H. Duroy, and J. L. Fourquet, *Mater. Res. Bull.* **23,** 447 (1988).
11. H. Rietveld, *J. Appl. Crystallogr.* **2,** 65 (1969).
12. A. C. Larson and R. B. Von Dreele, Los Alamos Laboratory Report LA-UR-86-748, 1987.
13. P. Main, MULTAN84, University of York, UK, 1984.
14. Y. Le Page and E. Gabe, NRCVAX, National Research Council, Canada 1984.
15. C. Baerlocher, *in* "The Rietveld Method" (R. Young, Ed.), pp. 186–196. Oxford Univ. Press, New York (1993).
16. K. Schunemann and K. M. Mueller-Buschbaum, *J. Inorg. Nucl. Chem.* **37,** 1879 (1975).
17. B. Morosin and R. W. Lynch, *Acta Crystallogr. B* **28,** 1040 (1972).
18. S. Geller and V. B. Bala, *Acta Crystallogr.* **9,** 1019 (1956).
19. M. Gasperin, M. C. Saine, A. Kahn, F. Laville, and A. M. Lejus, *J. Solid State Chem.* **54,** 61 (1984).
20. N. Iyi, S. Inoue, S. Takekawa, and S. Kimura, *J. Solid State Chem.* **54,** 70 (1984).
21. M. A. Estermann, L. B. McCusker, and C. Baerlocher, *J. Appl. Crystallogr.* **25,** 539 (1992).